**Supplementary Information**

---

**Contents**

## Experimental

***Materials.*** Acetic acid (reagent grade, ≥ 99.0 %), diethyl ether, deionized water, methanol (puriss p.a., absolute, ≥ 99.8 % (GC)), 4-ethynylaniline (97.0 %), p-toluenesulfonic acid monohydrate (ACS reagent, ≥ 98.5 %), 4-azidobenzoic acid solution (~0.2 M), gold(III) chloride trihydrate (99.995 %), tri-sodium citrate dihydrate, TEMPO (>98.0 %), cyclooctatetraene (98.0 %), Cyclohexene (analytical standard), 4-Cyanobenzoic acid (99%), Poly(ethylene glycol) (PEG, $M_n \approx 400$) were purchased from Sigma-Aldrich and used without further purification. Biotin azide (PEG4 carboxamide-6-azidohexanyl biotin) was purchased from Thermo Fisher.

***Preparation of AuNPs.*** Gold nanoparticles were prepared by a modified Turkevich method [S1]. In 250 mL round bottomed flask, 1 mL of $HAuCl_4$ (100 mg in 10 mL) and 2.5 mL of $Na_3CA$ (284.9 mg in 25 mL) were added to 100 mL of boiling water. Heating was continued for 10 min during which time the solution become red. After cooling to room temperature, the nanospheres solution was used as prepared.

***Preparation of AuNPs-C≡CH and AuNPs-N3.*** 4-ethynylbenzenediazonium tosylate (ADT-C≡CH) was synthesized according to the published procedure [S2]. 40 ml of as prepared AuNPs were mixed with 10 ml of 1mM solution of ADT-C≡CH or ADT-$N_3$ for 40 min under magnetic stirring. After modification AuNPs were washed by water (2x), methanol (3x), acetonitrile and 5 ml of resulting suspension in acetonitrile was used for the experiments. Synthesis of 4-azidobenzenediazonium tosylate (ADT-N3) was performed according to [S3].

***AAC in viscous solution.*** For the preparation of reaction mixture with increased viscosity (0.67 mPa), 1 ml of suspension of AuNPs-C≡CH in acetonitrile was mixed with 2 ml of 1 mM solution of 4-azidobenzoic acid and 0.5 ml of polyethylene glycol (PEG, $M_n \approx 400$). The resulting suspension was illuminated for 3 hours with LEDs (660 nm, 20 mW/mm$^2$) at 23 °C. After reaction, AuNPs were isolated by centrifugation and analysed in the same manner as described above.

***Control reaction under 405 nm LED***. 0.1 mmol of phenylacetylene (11 µl) was mixed with 0.1 mmol of 4-azidobenzoic acid (0.5 ml 0.2 M solution) and the resulting mixture was illuminated for 3 hours with light-emitting diode (LED) (405 nm emission wavelength) in controlled temperature chamber at -35 °C under magnetic stirring. The resulting mixture was analysed by Agilent 7010 GC was equipped with a flame ionisation detector (FID) and a Rxi-5ms column (20 m x 0.18 mm x 0.30 um). GC program: 40°C (5 min) - > 45°C/min - > 230°C (5 min), carrier gas: Helium, constant flow 0.9 ml/min, injection volume: 1 µl, split 1:10, inlet temperature 250°C.

***Control copper-catalysed reactions.*** 1 ml of suspension of AuNPs with attached 4-ethynylphenyl groups in acetonitrile was mixed with 2 ml of 1 mM solution of 4-azidobenzoic acid followed by addition of sodium ascorbate (0.03 mmol, 100 µL of freshly prepared 3 M solution in

water) was added and copper(II) sulfate pentahydrate (0.03 mmol, 7.5 mg). Resulting mixture was mixed with magnetic stirrer for definite time periods in controlled temperature chamber under magnetic stirring.

***Control SERS measurement of biotin-azide.*** As prepared citrate stabilised AuNPs (10 ml) were washed by water and methanol, and redispersed in 1 ml of methanol. 0.1 ml of resulting suspension was deposited on the silica substrate (0.5 cm×0.5 cm) and dried at room temperature. The solution of biotin-azide (1 mg/ml) was drop deposited on AuNPs array, left dried at 3 °C and subjected to further SERS measurement.

***Measurement techniques.*** UV-Vis spectra were measured using Spectrometer Lambda 25 (Perkin-Elmer) in 300-1000 nm wavelength range. Raman spectra were recorded using ProRaman-L spectrometer (785 nm excitation wavelength, 35 mW power). Excitation and collection of the resulting Raman scattered light was done using a 40× microscopic objective in 180$^{o}$ measurement geometry. Spectra accumulation time was 100 s. All spectra were baseline corrected and smoothed using an 11-point averaging to reduce the baseline variability at the region between 450 and 2500 $cm^{-1}$, using Omnic Professional Software Suite (Thermo Scientific, Inc., Madison, WI). Light irradiance on sample surface was measured with Integrating Sphere Photodiode Power Sensors (Thorlabs, S142C), taking into account the laser spot diameter, and found to be 25 $mW/cm^2$. TEM images of nanoparticles were obtained on JEOL JEM-1010 instrument operated at 80 kV (JEOL Ltd., Japan).

A Brookfield rheometer DV3T was used for measurement of reaction mixture viscosity in -40 – 25 $^{o}$C temperature range. The experiments were performed in controlled temperature chamber Binder MK 56 using the pristine acetonitrile or AuNPs-C≡CH suspension in acetonitrile. The measurements were repeated five times for each temperature.

The dynamic light scattering measurements were performed with Malvern Zetasizer Ultra device before and after AuNPs-C≡CH suspension cooling/heating cycle. In the case of temperature-controlled experiments the UV-Vis spectra were obtained in back-reflected mode (200 nm thick Ag layer was evaporated onto the bottom of the cuvette), using the optical fiber connected to HR2000 (Ocean Optics) spectrometer and AvaLight-DHS light source.

***A list of control experiments:***

1 ml of suspension of AuNPs with attached 4-ethynylphenyl groups (or other if specified) in acetonitrile was mixed with 2 ml of 1 mM solution of 4-azidobenzoic acid and resulting mixture was illuminated for 3 hours with light-emitting diode in controlled temperature chamber under magnetic stirring. After reaction, the modified AuNPs were separated by centrifugation (7000 rpm, 20 min),

washed by acetonitrile and methanol, and dispersed in methanol to the final volume 0.5 ml. 0.1 ml of resulting suspension was deposited on the silica substrate (0.5 cm×0.5 cm), dried at room temperature and subjected to further SERS analysis. Specification of control experiment is presented below, all experiments were repeated 3 times:

1. AAC without LED illumination,
2. AAC with illumination by 405 nm LED (1050 mW),
3. AAC with the addition of TEMPO ($10^{-6}$ M) at RT and -35 °C under plasmon-assistance (660 nm LED irradiation),
4. AAC with the addition of COT ($10^{-6}$ M) at RT and -35 °C under plasmon-assistance (660 nm LED irradiation),
5. AAC with the addition of cyclohexene ($10^{-4}$ M) at RT and -35 °C under plasmon-assistance (660 nm LED irradiation),
6. AAC with the addition of 4-cyanobenzoic acid ($10^{-4}$ M) at RT and -35 °C under plasmon-assistance (660 nm LED irradiation),
7. AAC with the addition of AuNPs with grafted 4-azidophenyl groups and phenylazide at -35 °C under plasmon-assistance (660 nm LED irradiation).
8. Influence of solution viscosity: AAC at RT with addition of PEG (suspension viscosity was adjusted to value 0.67 mPa, corresponding to viscosity of ACN at -35$^{o}$C)
9. AuNPs agglomeration under decreased temperature and estimation of plasmon heating in reaction progress.

**Table S1**

Raman Peak Frequencies and Assignments for AuNPs modified by ADT-C≡CH before and after AAC plasmon-induced reaction.

| **Raman Peak Frequencies and Assignments for AuNPs-C≡CH ($cm^{-1}$)** | | **Raman Peak Frequencies and Assignments for AuNPs-C≡CH after plasmon-induced AAC ($cm^{-1}$)** | |
|---|---|---|---|
| **2000** | C≡C stretch | **2235** | N=N stretch |
| **1590, 1486, 1430** | Ar (C=C) vibration | **1590** | Ar (C=C) vibrations |
| **1150, 1111, 1036** | C-H in plane deformation of Ar | **1550** | C=O stretch (from COOH) |
| **682,627** | C-H out plane deformation of Ar, Ar (C=C) vibration | **1392, 1315, 1193, 1105, 1024** | triazole ring |
| **509** | C≡CH stretch | **906** | C–H wagging |
| **401** | Au-C stretch | **822** | CH deformation of Ar |
| | | **771** | Ar ring torsion |
| | | **682** | C–H wagging |
| | | **640** | N–H waging |

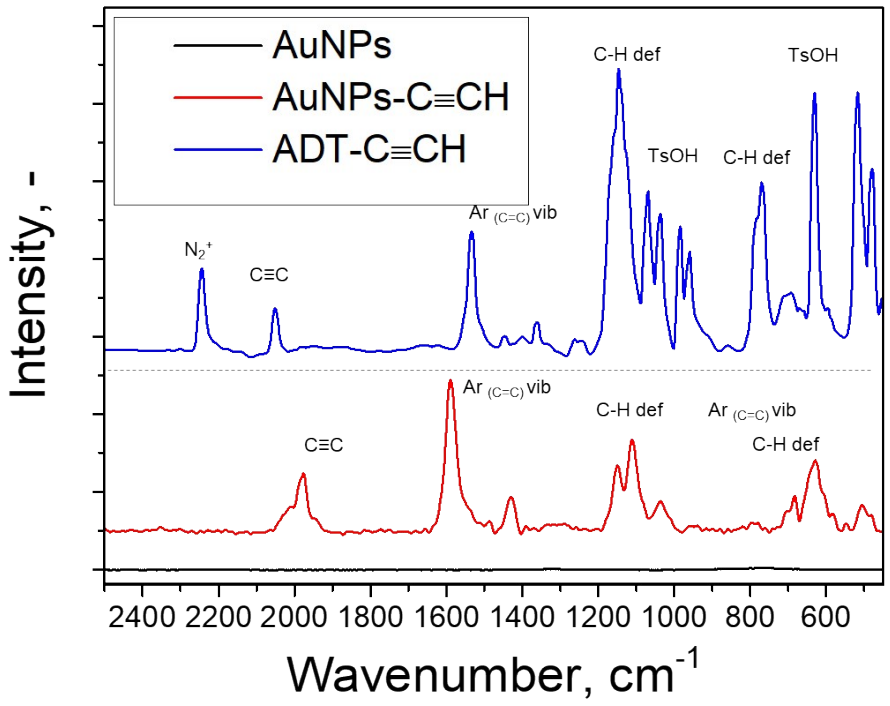


**Figure S1** Raman spectrum of ADT-C≡CH powder and SERS spectra of pristine AuNPs and AuNPs after grafting with ADT-C≡CH (i.e. AuNPs with attached 4-ethynylphenyl groups).

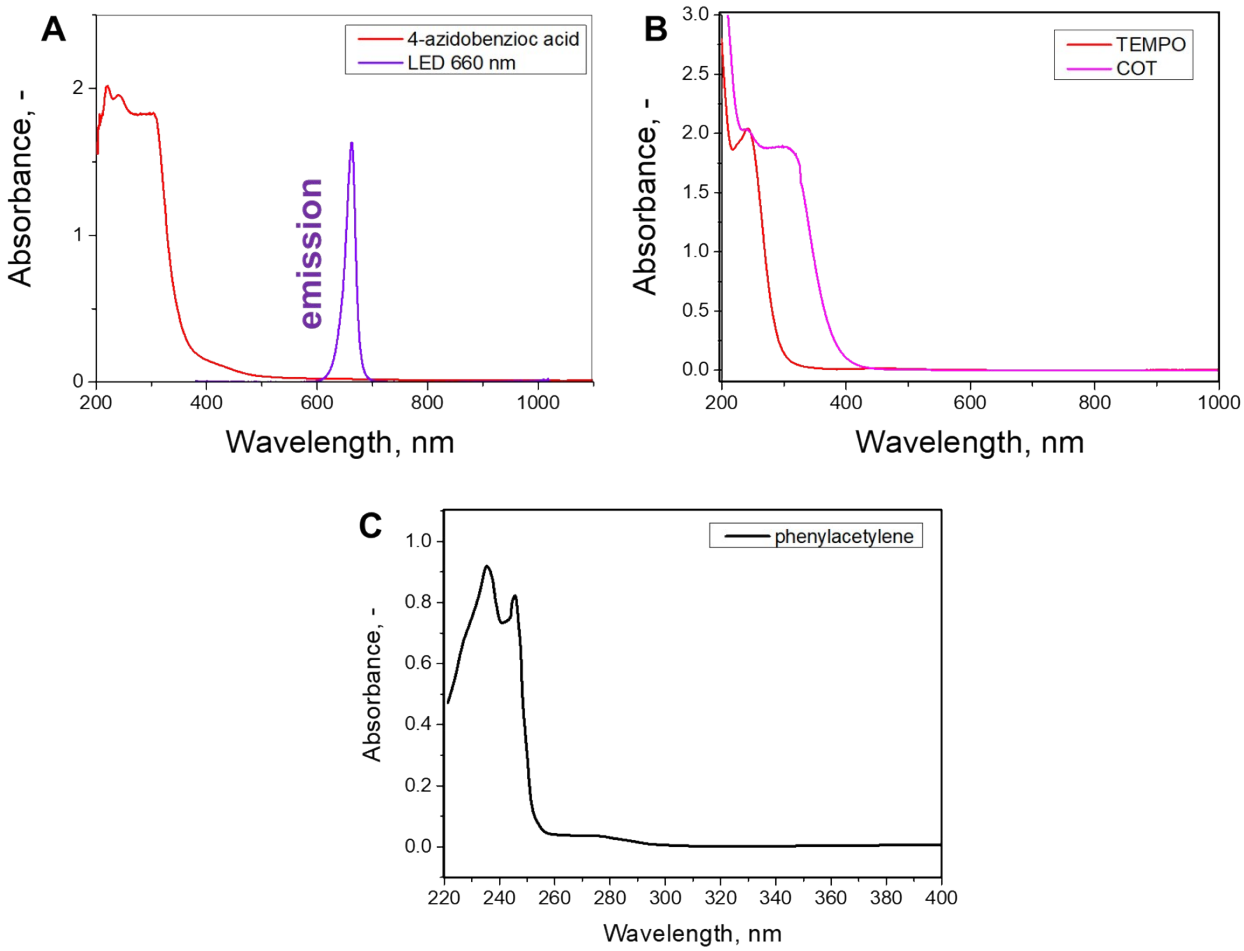


**Figure S2** UV-Vis spectra of: (A) - 4-azidobenzoic acid, (B) - TEMPO and COT, and (C) – phenylacetylene (solutions in acetonitrile were used for measurements).

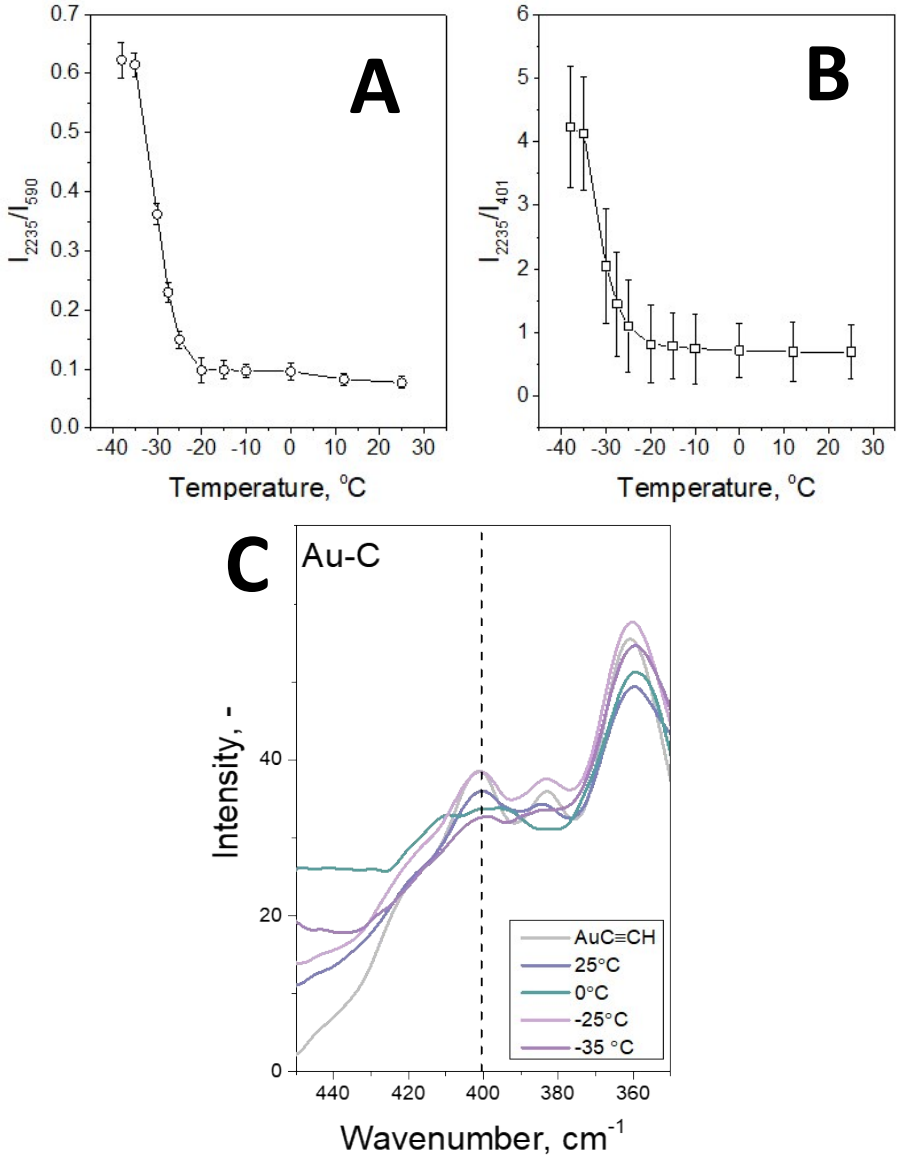


**Figure S**3 Dependence of reaction conversion estimated as increase of $I_{2235}/I_{1590}$ (A) and $I_{2235}/I_{401}$ (B) SERS peak ratios on the temperature; (C) – deviation of characteristic Au-C peak intensity.

***Figure S3 – related discussion.*** Since the $I_{1590}$ signal from benzene ring can not be considered as constant and will increase with AAC progress, we also present the $I_{2235}/I_{401}$ peak ratio (the SERS band at 401 cm$^{-1}$ is attributed to Au-C vibration, which is not dependent on reaction progress. Characteristic $I_{2235}/I_{401}$ SERS peak ratio is presented in Fig. S3 as a function of reaction temperature (in comparison with $I_{2235}/I_{1590}$ peaks ratio). In addition, the spectra range 350-450 cm$^{-1}$, related to Au-C characteristic vibration (extracted from spectra data), is presented in Fig. S3C. As is evident, utilisation of Au-C or benzene-ring vibrations as a SERS marker produce similar results - rapid increase of observed conversion, which becomes especially pronounced in -20 °C to -30 °C temperature range. Moreover, the "absolute" increase was larger when reaction progress was normalised by Au-C band SERS intensity. On the other hand, the absolute intensity of Au-C vibration is large (Fig. S3C) and it

partially overlaps with other vibration bans (Fig. 2 – main manuscript text). Thus we prefer to utilise of $I_{2235}/I_{1590}$ peaks ratios to make some quantitative conclusion about the reaction progress at a decreased temperature.

## Kinetic Experiments

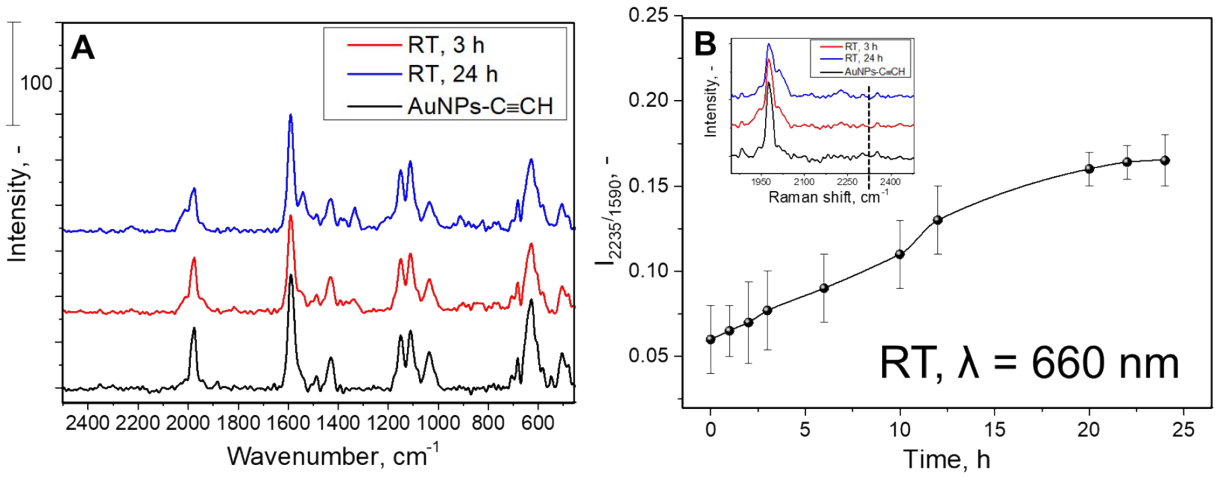


**Figure S4** (A) - SERS spectra of Au-C≡CH before and after plasmon induced AAC at RT, (B) - corresponding kinetic of triazole formation

***Figure S4 – related discussion.*** In order to establish the reaction time required for the comparison on SERS spectra of AuNPsC≡CH after reaction at different temperature we perform kinetic SERS measurements at RT. We monitored the reaction through the registration of triazole-related peak appearance (at 2235 $cm^{-1}$ – see Tab. S1). After 3 hours of reaction we observed formation of well-visible spectral changes, therefore this time was chosen for the evaluation of temperature effect on the reaction rate.

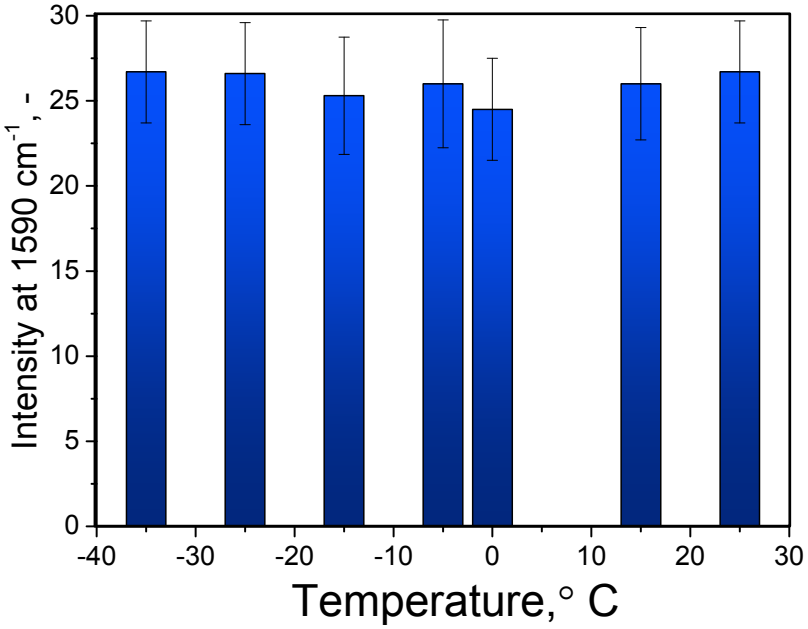


**Figure S5** SERS intensity of peak at 1590 $cm^{-1}$ (Ar ring mode) from grafted 4-ethynylphenyl groups, measured after AuNPs-C≡CH illumination with 660 nm wavelengths at different temperatures in acetonitrile.

***Figure S5 – related discussion.*** In order to exclude the degradation of organic layer on AuNPs, we recorded the intensity of peak at 1590 $cm^{-1}$ on AuNPs-C≡CH after storing at different temperature for 3 hours in acetonitrile under LED illumination (660 nm). This peak is related to aromatic ring, which does not participate in AAC reaction and can be used for estimation of decomposition or detachment of grafted 4-ethynylphenyl moieties. Obtained results are presented in Fig. S5 (as an averaged value of peaks intensity, obtained in SERS measurements on different samples and spots, error bars corresponded to the standard deviation between measurements). Conservation of averaged peak intensity (with regard to typical SERS uncertainty) allows us to claim, that the decomposition or detachment of grafted organic moieties does not occur.

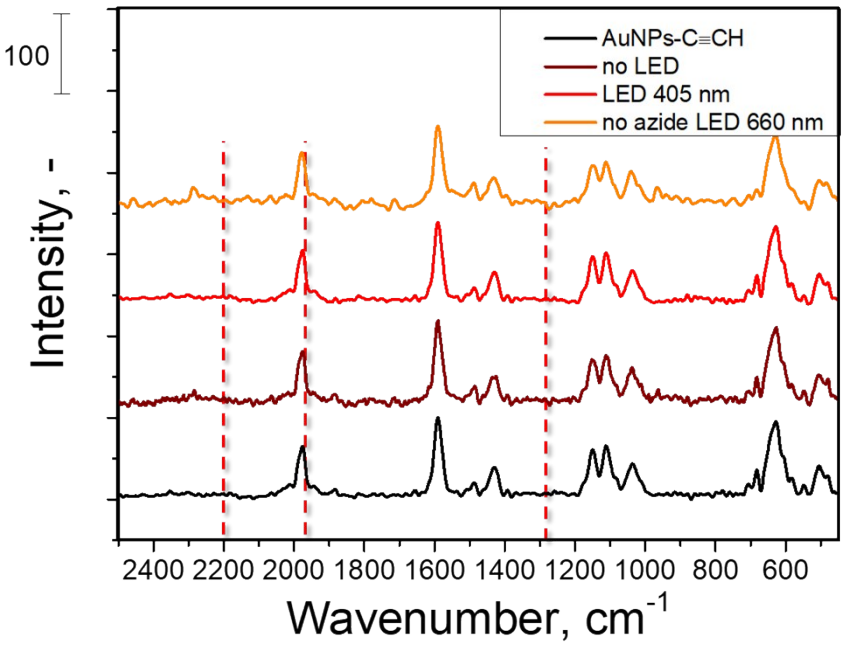


**Figure S6** SERS spectra from control experiments: absence of light irradiation, irradiation of AuNPsC≡CH – azide mixture with 405 nm wavelength, absence of azide in reaction mixture (assignments of peaks are presented in Tab. S1).

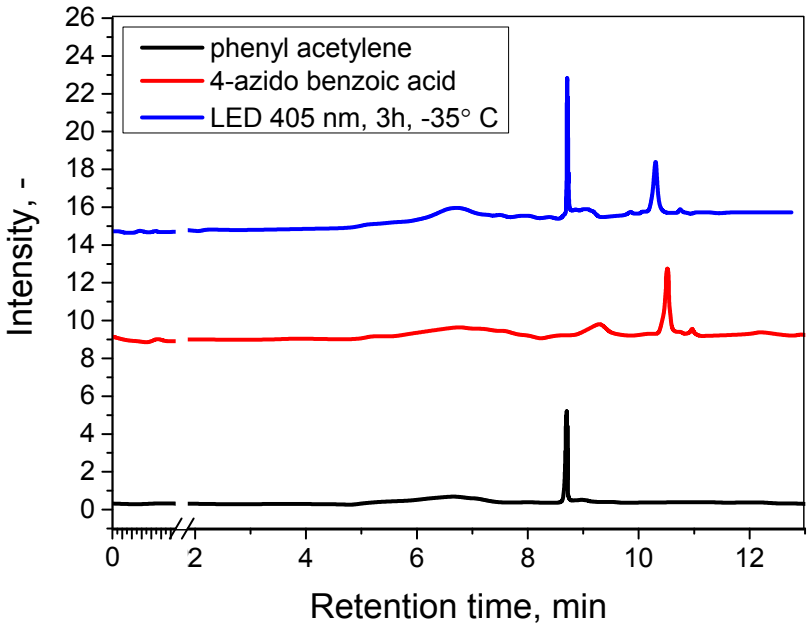


**Figure S7** GC chromatogram obtained from phenylacetylene, 4-azidobenzoic acid and after their mixture irradiation at 405 nm excitation wavelength for 3 hours at -35 °C

***Figures S6, S7 – related discussion.*** In order to prove the plasmonic nature of performed chemical transformations, we conducted the range of control experiments: (i) AAC without

illumination (dark), using LED 405 nm (this wavelength is out of absorbance of AuNPs in acetonitrile) and the illumination of AuNPs-C≡CH without azide addition. Reaction proceeding was estimated by SERS, and GC (after separation and washing of AuNPs-C≡CH) and obtained results are presented in Figs. S6 and S7. In the first case, we did not find any spectral difference between SERS spectra, measured on AuNPs-C≡CH before and after reaction. Thus, we can conclude that AAC occurs only under plasmon assistance, i.e. when the AuNPs with grafted 4-ethynylphenyl are dispersed in azide solution and illuminated with wavelength corresponded to plasmon absorption band. In turn, from Fig. S7 we can conclude that illumination of phenylacetylene and 4-azido benzoic acid without the initiation of plasmon on AuNPs does not lead to AAC proceeding.

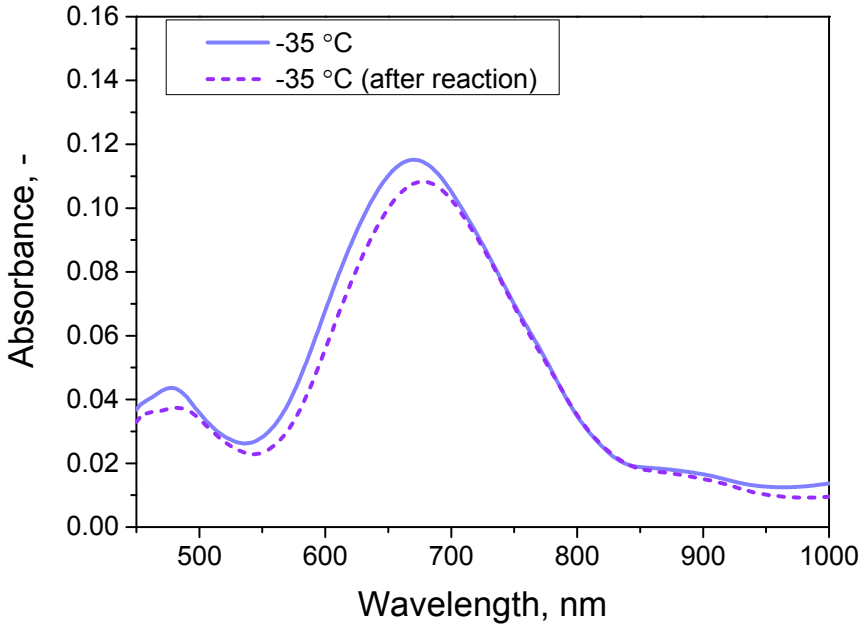


**Figure S8** UV-Vis of AuNPs–C≡CH in acetonitrile cooled to -35 °C and after 3 hours of irradiation in the presence of azide and washing with acetonitrile.

***Figures S8 – related discussion.*** We also measured UV-Vis spectra of AuNPs–C≡CH after the reaction with 4-azidobemzoic acid in optimal conditions and following washing with acetonitrile. The intensity of gold absorption decreased insignificantly, no plasmon band widening was observed, indicating the absence of nanoparticle agglomeration. The slight shift of plasmon band position can be attributed to AAC proceeding and related changes of gold nanoparticles dielectric environments

## Estimation of potential plasmon heating and local temperature near the AuNP and AuNPs (dimer case) surface.

The calculation of local heating produced by illuminated AuNPs dimer was performed in assumption of steady-state illumination with 660 nm wavelength and light fluency, corresponding to conditions used in our experiments. First, the calculation of AuNP and subsequently AuNPs dimer absorption cross-section was performed in the framework of Generalized Mie theory, implemented in the py_gmm software [S4]. For dimer, we focused attention on 0.7 nm gap between AuNPs (taking into account the grafted dielectric layer between nanoparticles), since in this plasmonic hot spot the highest electric field concentration and related Joule heat production can be expected. The "minimal" gap between two nanoparticles was estimated from the size of grafted organic moieties (-*p*-$C_6H_4$-C≡CH).

First, we considered the single nanoparticle case. The calculation of local heating produced by illuminated AuNP was performed in an assumption of steady-state illumination and light fluency, corresponding to conditions used in our experiments. Determined from generalized Mie theory absorption cross-section was used to calculate local heating near nanoparticle surface, under the assumption of homogeneous heat generation in the whole NP volume (this approach is commonly used for calculation of local heating produced by illuminated MeNPs due to their small size and high thermal bulk conductivity). The calculation was performed according to the semi-analytical solution of the heat flow from the sphere in an infinite medium, derived by Goldenberg and Tranter [S5, S6]. It was found, that under experimental condition temperature elevation in the close vicinity of nanoparticle surface is in the order of $10^{-3}$ K (Fig. S9). Indeed, this value is insignificant and thus, local heating effect can be neglected in single spherical AuNP case.

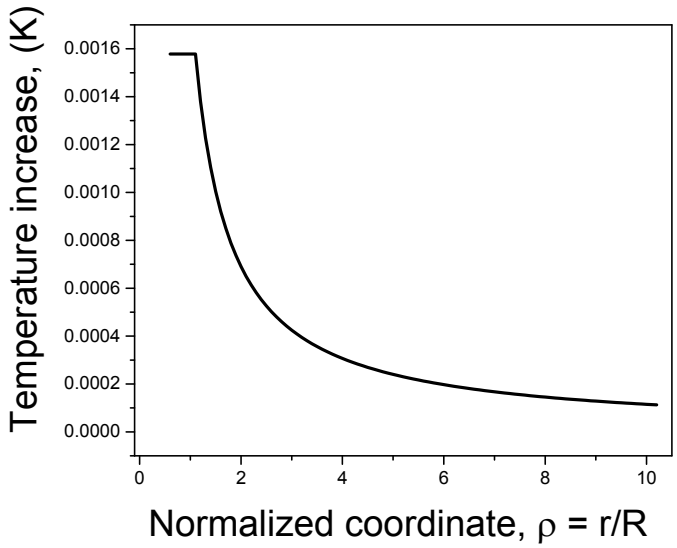


**Figure S9** Calculated local increase of temperature near AuNP surface (nanoparticle diameter – 25 nm, acetonitrile was used as dielectric environment) under the continuous illumination (660 nm, irradiance - 20 mW/mm$^2$).

Second, we consider the case of nanoparticles dimer. In this case, the collective effects indeed may lead to significant enhancement of local heating, The irradiance is so low that even obtained results could not be justified by local effects. To demonstrate that we calculated distribution of heat power density inside nanoparticle dimer using volume-integral-equation solver BUFF-EM [S5, S6]. The finite-element mesh with linearly increasing mesh density towards inter-particle gap was generated with GMSH mesher (shown in Fig. S10A). Resulting heat power density was normalized by mean power density (which was assumed in the previous case of single AuNP). The deviation from single AuNPs is presented in Fig. S10B. Maximal heat power generation (observed in the vicinity of gap) was 264 times greater than the average value for single nanoparticle. This enhancement of local heating is indeed significant, but even neglecting enhanced heat transfer to colder surrounding in case of nonuniform heat generation (i.e. supposing that whole volume of nanoparticle generates 264 times more heat) the local temperature enhancement is still below 1 K, which is still not enough to justify all observable effects of AAC enhancement under plasmon initiation.

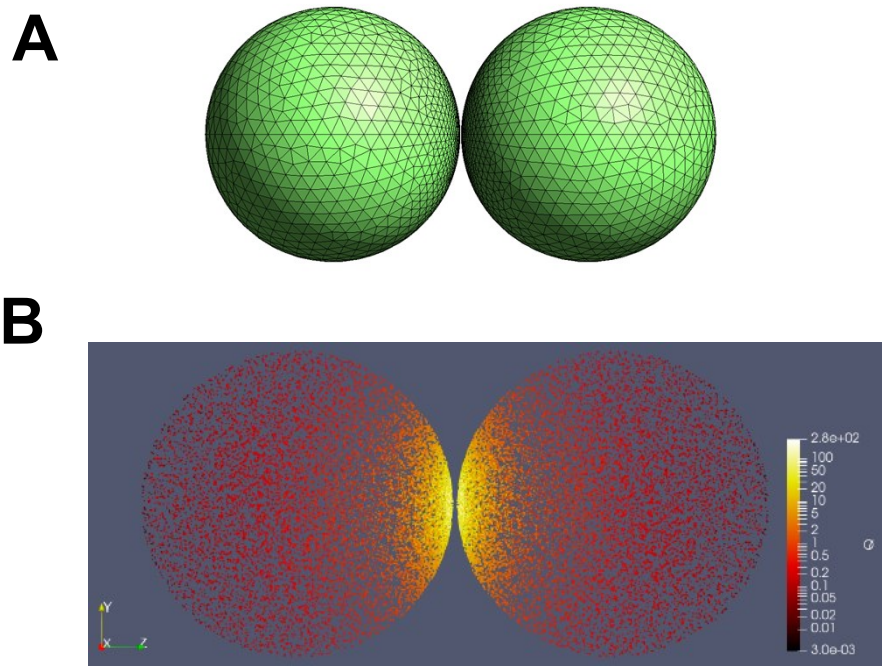


**Figure S10** (A) - System meshing, used for numerical simulation; (B) – Calculated heat power density distribution (heat power density in "plasmonic gap" is normalized by mean power density).

## Estimation of plasmon-excited electron lifetime under the reaction mixture cooling

According to [S7] the Drude damping parameter ($\gamma_p$) defines the mean lifetime (approximated by the momentum relaxation time) $\tau$ and hot electrons generation efficiency $R_{he}$, both of which being inversely proportional to $\gamma_p$. Thus, we can reduce analysis of the temperature dependence of hot-electron generation and mean lifetime to the analysis of temperature dependence of the parameter $\gamma_p$, which was investigated in [S8]. In short, the damping parameter is decomposed into two parts electron-electron and electron-phonon contributions $\gamma_p = \gamma_{e-e} + \gamma_{e-ph}$. The $\gamma_{e-e}$ contribution is significant only during the first stage (very short) of plasmon-excited electrons relaxation (or at very low temperatures) and thus can be neglected. The electron-phonon interaction were described by Holstein [S9] as

$$\gamma_{e-ph} = \gamma_0 \left( \frac{2}{5} + 4\frac{T^5}{\theta_D^5} \int_0^{\frac{\theta_D}{T}} \frac{z^4}{e^z - 1} dz \right),$$

where $\theta_D$ is Debye temperature and $\gamma_0$ is experimental constant. Since we are interested only in ratio $\frac{\gamma_{e-ph}(T_0)}{\gamma_{e-ph}(T_1)}$ the constant does not play a role. Finally, by computing this ratio for $T_0 = 298$K, $T_1 = 238$K the ratio $\frac{\tau(T_1)}{\tau(T_0)} = \frac{R_{he}(T_1)}{R_{he}(T_0)} = 1.240$ was obtained.

## Control Experiments

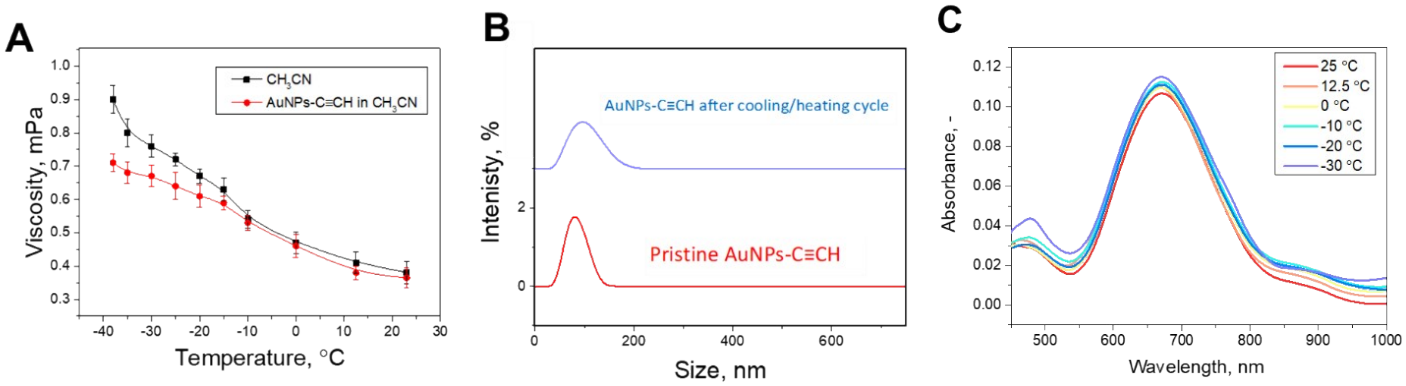


**Figure S11** (A) – Changes of the viscosity of acetonitrile and suspension of AuNPs-C≡CH with temperature decrease; (B) – Dynamic light scattering measurements of AuNPs-C≡CH suspension in acetonitrile, performed before and after cooling/heating cycle; (C) – UV-Vis absorption spectra of AuNPs-C≡CH suspension in acetonitrile, measured at various temperatures.

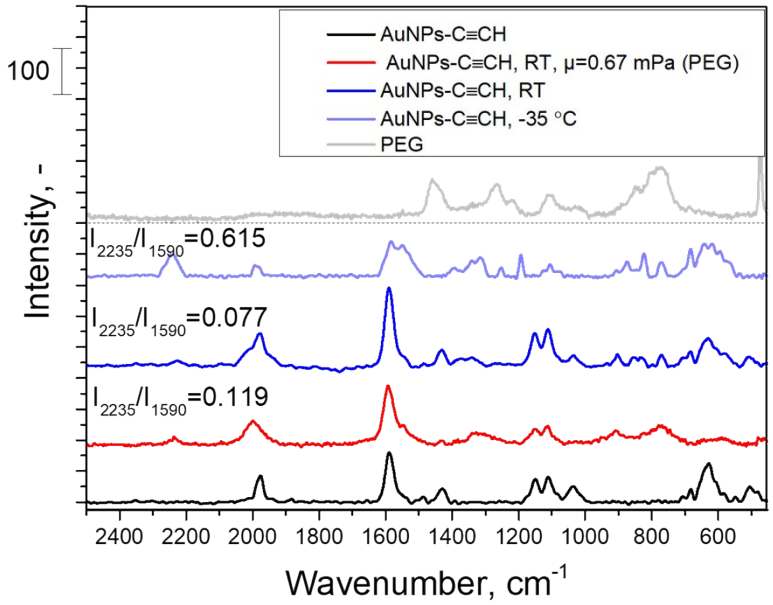


**Figure S12** SERS spectra measured after plasmon-induced AAC at different conditions: decreased temperature, room temperature, and room temperature with PEG addition to reaction mixture (viscous reaction mixture). The SERS spectrum of pristine AuNPs-C≡CH and Raman spectrum of PEG are presented for comparison.

***Figure S11, Figure S12 – related discussion*** In order to exclude the potential impact of the viscosity increase under reaction mixture cooling (and related nanoparticles agglomeration) we performed the range of control experiments:

First, the viscosities of acetonitrile and AuNPs-C≡CH suspension in acetonitrile were measured under cooling (Fig. S11A). As can be expected, the cooling results in a viscosity increase in both cases. In the second step, we adjusted the viscosity of reaction mixture at RT to value, measured at T = -35 $^{o}$C by addition of PEG (14% vol.) and performed the plasmon-initiated AAC at room temperature in acetonitrile/PEG mixture. Commonly, the PEG molecules are absorbed on the surface of metal nanoparticles, but in our case, the surface of AuNPs is already coated with –*p*-$C_6H_4$-C≡CH chemical moieties, which should prevent PEG adsorption. Results of AAC are presented in Fig. S12, and absence of apparent PEG peaks is evident on AuNPs surface (the PEG spectrum is also presented for comparison). The AAC progress was also estimated from characteristic SERS bands ratio ($I_{2235}/I_{1590}$). In the case of PEG addition, the peaks ratio was founded to be slightly increased, compared to pristine reaction mixture (0.119 vs 0.077). However, the observed increase is far below, than observed in the case of reaction mixture cooling (0.615 vs 0.077). Thus, we can conclude that viscosity increase under reaction mixture cooling cannot explain the reaction progress enhancement and observed phenomenon should be attributed to the nature of plasmon catalysis.

In turn, Fig. S11B and Fig. S11C show the UV-Vis spectra of AuNPs-C≡CH as a function of temperature decrease and size distribution of AuNPs-C≡CH measured by DLS before and after suspension cooling to -40 $^{o}$C, keeping at this temperature for 3 h and slowly heating again to RT. The UV-Vis spectra do not demonstrate any apparent changes in the position or half-width of the plasmon absorption band, indicating the absence of pronounced nanoparticle agglomeration. Performed DLS measurements show slightly broadening of Au-NPs size distribution and certain increasing of average nanoparticles diameter (Fig. S11B). So, taking into account the potential impact of nanoparticles agglomeration on the increasing of local plasmon heating, we performed the numerical simulation of heat generation in AuNPs dimer (discussed above).

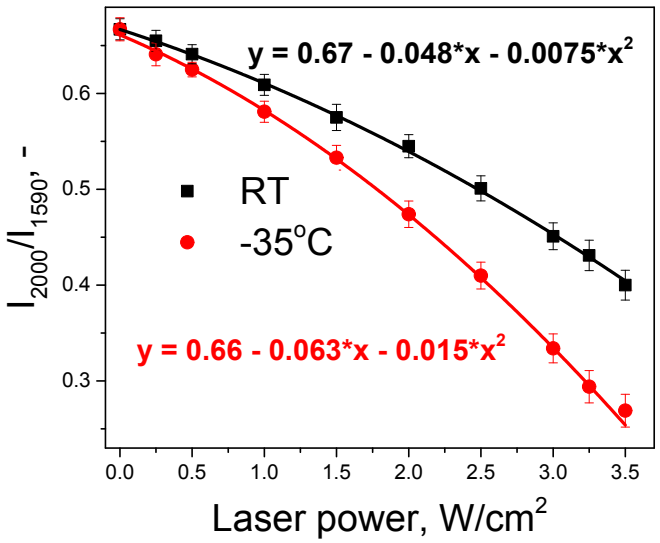


**Figure S13** Nonlinearly fitted dependencies of AAC conversion on the laser power at room and decreased temperature.

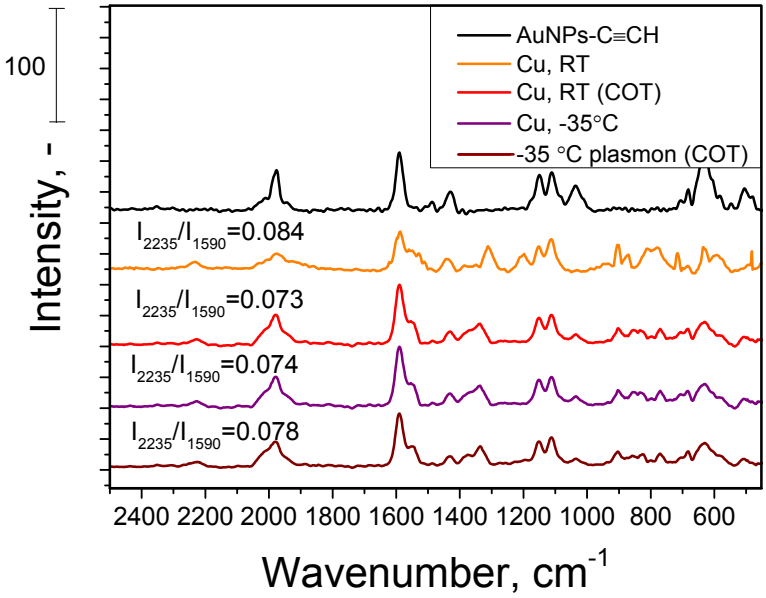


**Figure S14** Control experiments: (A) - SERS spectra measured on AuNPs-C≡CH before and after AAC (initiated by common Cu-catalyst or plasmon triggering) in COT presence at room and decreased temperature;

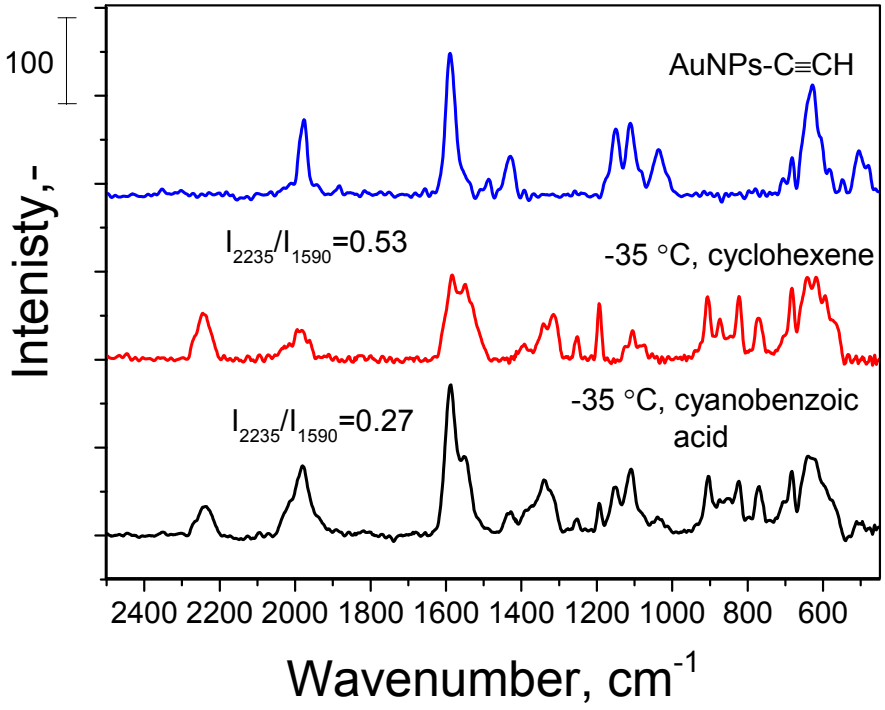


**Figure S15** Control experiments – impact of addition of cyclohexene ($10^{-4}$ M) or 4-cyanobenzoic acid ($10^{-4}$ M) to reaction mixture (plasmon-induced AAC, -35°C).

***Figure S15 – related discussion***. To further estimate the impact of COT (which block the plasmon assistance in AAC) we performed the range of alternative experiments with addition of cyclohexene or 4-cyanobenzoic acid. These compounds can be potentially adsorbed to grafted AuNPs surface (and block the acetylene groups, like COT), but do not work as triplet excited state scavenger (unlike COT). Obtained results (estimated by SERS) are presented in Fig. S15 and shows that addition of cyclohexene does not affect the reaction rate to such extent as COT (SERS spectra were measured after reaction proceeding under the plasmon excitation at -35°C). We observed the moderate inhibition of the reaction with 4-cyanobenzoic acid addition, which may be attributed to partial blockage of surface reaction sites. It should be noted that concentration of added cyanobenzoic acid was two orders of magnitude larger than COT concentration, which completely block the plasmon-triggered AAC proceeding. So, we can conclude that AAC reaction blocking by COT should be attributed to quenching of plasmon-induced triplet state(s) or triplet state transfer, but not to the blocking of grafted nanoparticles surface.

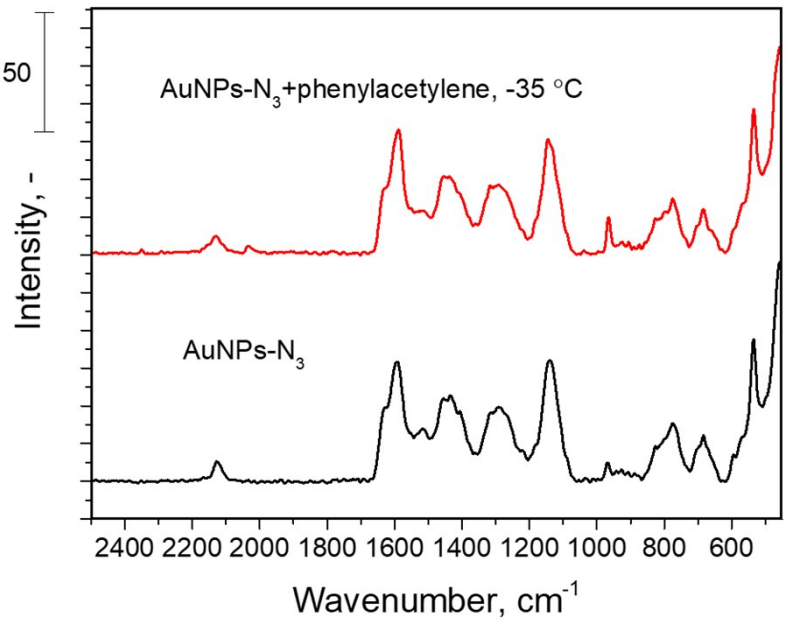


**Figure S16** Control experiments – ability of "reverse" plasmon initiation: SERS spectra measured on AuNPs grafted with phenylazide before and after the reaction with phenylacetylene in acetonitrile at -35 °C under plasmon assistance. Conservation of spectral features and absence of new characteristic bands indicate that under this condition AAC does not proceed.

**Table S2** Raman Peak Frequencies and Assignments for Biotin azide and AuNPs-Biotin after plasmon-induced AAC reaction (additional peaks)*.

| **Biotin azide** | |
|---|---|
| Wavenumber, $cm^{-1}$ | Assignment |
| 2097 | $N_3$ asym str |
| 1706 | C=O str |
| 1690 | C=O str |
| 1670 | N-H def |
| 1638 | N-H def |
| 1550 | N-H def |
| 1463 | $CH_2$ scis vib, CH def vib |
| 1263 | C-N str, CH def vib |
| 1124 | CH in plasne vib |
| 1013 | CN str, C-C skel vib |
| 985 | $CH_2$ out of plane, C-C skel vib |
| 940 | C-C skel vib |
| 752 | C-S str |

| | |
|---|---|
| 627 | C-S str |
| 525 | C-C skel vib, $CH_2$ rocking vib |
| **AuNPs-Biotin (additional peaks in comparison with pristine AuNPs-C≡CH)** | |
| Wavenumber, $cm^{-1}$ | Assignment |
| 2102 | Triazole ring |
| 1644 | C=O str |
| 1617 | N-H def |
| 1547 | N-H def |
| 1336 (1264-1403) | Triazole ring |
| 901 | C-C skel vib |
| 747 | C-S str |
| 635 | C-S str |
| 509 | C-C skel vib, $CH_2$ rocking vib |

*Peaks assignment according to [S10 –S12]

## References


[S1] Shiv Shankar, S.; Bhargava, S.; Sastry, M. Synthesis of Gold Nanospheres and Nanotriangles by the Turkevich Approach. *J. Nanosci. Nanotechnol.* **2005**, *5* (10), 1721–1727. https://doi.org/10.1166/jnn.2005.192.

[S2] Guselnikova, O.; Olshtrem, A.; Kalachyova, Y.; Panov, I.; Postnikov, P.; Svorcik, V.; Lyutakov, O. Plasmon Catalysis on Bimetallic Surface - Selective Hydrogenation of Alkynes to Alkanes or Alkenes. *J. Phys. Chem. C* **2018**, *122* (46), 26613–26622. https://doi.org/10.1021/acs.jpcc.8b07398.

[S3] Guselnikova, O.; Postnikov, P.; Chehimi, M. M.; Kalachyovaa, Y.; Svorcik, V.; Lyutakov, O. Surface Plasmon-Polariton: A Novel Way to Initiate Azide-Alkyne Cycloaddition. *Langmuir* **2019**, *35*, 6, 2023–2032

[S4] Pellegrini, G.; Mattei, G.; Bello, V.; Mazzoldi, P. Interacting Metal Nanoparticles: Optical Properties from Nanoparticle Dimers to Core-Satellite Systems. *Mater. Sci. Eng. C* **2007**, *27* (5-8 SPEC. ISS.), 1347–1350. https://doi.org/10.1016/j.msec.2006.07.025.

[S5] Homer Reid, M.~T. et al. "Efficient Computation of Power, Force, and Torque in BEM Scattering Calculations". *arXiv:1307.2966*. (2013).

[S6] Geuzaine, Christophe, and Jean-François Remacle. "Gmsh: A 3-D finite element mesh generator with built-in pre- and post-processing facilities." *Internat. J. Numerical Methods Engineer.* 79.11 (2009): 1309-1331.

[S7] Besteiro, L. V.; Kong, X. T.; Wang, Z.; Hartland, G.; Govorov, A. O. Understanding Hot-Electron Generation and Plasmon Relaxation in Metal Nanocrystals: Quantum and Classical Mechanisms. *ACS Photonics* **2017**, *4* (11), 2759–2781. https://doi.org/10.1021/acsphotonics.7b00751.

[S8] Beach, R. T.; Christy, R. W. Electron-Electron Scattering in the Intraband Optical Conductivity of Cu, Ag, and Au. *Phys. Rev. B* **1977**, *16* (12), 5277–5284. https://doi.org/10.1103/PhysRevB.16.5277.

[S9] Holstein, T. Theory of Transport Phenomena in an Electron-Phonon Gas. *Ann. Phys. (N. Y).* **1964**, *29* (3), 410–535. https://doi.org/10.1016/0003-4916(64)90008-9.

[S10] W. J. Tipping, M. Lee, V. G. Brunton, G. C. Lloyd-Jones and A. N. Hulme, *Faraday Discuss.*, 2019, **220**, 71–85.

[S11] K. Goodge and M. Frey, *Nanomaterials*, 2020, **10**, 1172.

[S12] G. Socrates, Infrared and Raman Characteristic Group Frequencies: Tables and Charts - George Socrates, 2204, p.50, 90, 117, 143, 209

## Reaction coordinates

14

**phenylacetylene** scf done: -308.512413 Sum of electronic and thermal Free Energies -308.433746 imag. freq.: 0

| | | | |
|---|---|---|---|
| C | -0.002280 | 0.000814 | -0.000146 |
| C | 0.001561 | 0.001082 | 1.405236 |
| C | 1.228668 | 0.000456 | 2.090390 |
| C | 2.424605 | -0.000417 | 1.380208 |
| C | 2.413936 | -0.000682 | -0.015191 |
| C | 1.198959 | -0.000064 | -0.701434 |
| C | -1.229143 | 0.001987 | 2.129816 |
| C | -2.268781 | 0.002817 | 2.741727 |
| H | 1.233452 | 0.000667 | 3.173657 |
| H | 3.366467 | -0.000891 | 1.916582 |
| H | 3.348004 | -0.001362 | -0.565125 |
| H | 1.186764 | -0.000265 | -1.785248 |
| H | -0.947175 | 0.001298 | -0.529931 |
| H | -3.187645 | 0.003896 | 3.282973 |

14

**phenylacetylene triplet $T_1$** scf done: -308.395897 Sum of electronic and thermal Free Energies -308.327012 imag. freq.: 0

| | | | |
|---|---|---|---|
| C | -0.006206 | -0.001927 | 0.008535 |
| C | -0.006735 | 0.007133 | 1.361619 |
| C | 1.223346 | 0.009183 | 2.110913 |
| C | 2.481914 | 0.001592 | 1.410566 |
| C | 2.534534 | -0.007584 | 0.058508 |
| C | 1.279337 | -0.009984 | -0.738829 |
| C | 1.306018 | -0.019145 | -2.094297 |
| C | 1.330359 | -0.027141 | -3.331808 |
| H | -0.927046 | -0.003471 | -0.561213 |
| H | -0.947851 | 0.013037 | 1.900501 |
| H | 1.202086 | 0.016338 | 3.192559 |
| H | 3.401134 | 0.003354 | 1.986032 |
| H | 3.477042 | -0.013277 | -0.474603 |
| H | 1.351341 | -0.034196 | -4.398102 |

14

**phenylacetylene singlet $S_1$** scf done: -308.496472 Sum of electronic and thermal Free Energies -308.276374 imag. freq.: 0

| | | | |
|---|---|---|---|
| C | -0.000412 | -0.000048 | 0.000160 |
| C | -0.000361 | -0.000146 | 1.423501 |
| C | 1.231495 | -0.000066 | 2.136554 |
| C | 2.427505 | 0.000847 | 1.475896 |
| C | 2.455149 | -0.016869 | 0.007585 |
| C | 1.170504 | 0.000855 | -0.704024 |
| C | 3.630759 | -0.090310 | -0.670322 |
| C | 4.708996 | -0.218906 | -1.291880 |
| H | 1.180916 | 0.006724 | -1.786577 |
| H | -0.946733 | 0.005123 | -0.528675 |
| H | -0.939119 | 0.008957 | 1.964816 |
| H | 1.215143 | 0.005092 | 3.220493 |

H 3.369656 0.006704 2.009170
H 5.609114 0.047583 -1.810818

14
**phenylacetylene radical anion $R_0^-$** scf done: -308.579929 Sum of electronic and thermal Free Energies -308.506359 imag. freq.: 0
C -0.000700 -0.000023 0.001915
C -0.003104 -0.003716 1.382772
C 1.230225 -0.000773 2.134468
C 2.449168 0.013577 1.359764
C 2.420810 0.017055 -0.020797
C 1.203271 0.006158 -0.734009
C 1.243346 -0.017755 3.515864
C 1.253455 0.182844 4.762778
H 3.399192 0.020048 1.883711
H 3.360308 0.028536 -0.566135
H 1.193115 0.005624 -1.817362
H -0.950336 -0.001873 -0.525693
H -0.943142 -0.010593 1.924428
H 1.266299 -0.501482 5.608404

17
**Azide** scf done: -584.624794 Sum of electronic and thermal Free Energies -584.543808 imag. freq.: 0
C -0.002521 0.000000 0.000558
C -0.000044 0.000000 1.387979
C 1.208083 0.000000 2.097148
C 2.419425 0.000000 1.392685
C 2.427759 0.000000 0.008146
C 1.215096 0.000000 -0.690357
C 1.250840 0.000000 3.575923
O 0.025682 0.000000 4.144739
N 1.312453 0.000000 -2.101228
N 0.272178 0.000000 -2.762323
N -0.600965 0.000000 -3.480088
O 2.268154 0.000000 4.240056
H 3.353398 0.000000 1.939739
H 3.359249 0.000000 -0.544047
H -0.943554 0.000000 -0.536849
H -0.941738 0.000000 1.920074
H 0.145551 0.000000 5.110180

31
**TS** scf done: -893.109715 Sum of electronic and thermal Free Energies -892.930247 imag. freq.: 1(-408.39)
C -0.004774 0.114647 0.016713
C 0.003363 0.014169 1.416090
C 1.231593 -0.102306 2.088097
C 2.423985 -0.116267 1.370609
C 2.409631 -0.006113 -0.020068
C 1.192675 0.112937 -0.692159
C -1.219363 0.048138 2.178597
C -1.972082 0.400086 3.092918
N -3.760788 -0.788391 2.832518

| | | | |
|---|---|---|---|
| N | -3.416735 | -1.340862 | 1.750059 |
| N | -2.457575 | -1.400884 | 1.095193 |
| C | -5.096117 | -0.472664 | 3.107378 |
| C | -6.135992 | -0.652029 | 2.182984 |
| C | -7.429156 | -0.292879 | 2.528105 |
| C | -7.703988 | 0.258661 | 3.787317 |
| C | -6.657175 | 0.437566 | 4.701374 |
| C | -5.363415 | 0.070758 | 4.372095 |
| C | -9.069428 | 0.658926 | 4.187919 |
| O | -9.992095 | 0.440469 | 3.225142 |
| O | -9.365682 | 1.138909 | 5.264394 |
| H | -2.364168 | 0.909701 | 3.944419 |
| H | 1.241288 | -0.183236 | 3.168373 |
| H | 3.365433 | -0.210804 | 1.899677 |
| H | 3.339928 | -0.014460 | -0.576333 |
| H | 1.174828 | 0.198738 | -1.772671 |
| H | -0.949102 | 0.196064 | -0.506428 |
| H | -4.554371 | 0.197312 | 5.080309 |
| H | -6.868987 | 0.859391 | 5.675544 |
| H | -8.228420 | -0.437229 | 1.813477 |
| H | -5.925794 | -1.075547 | 1.208478 |
| H | -10.855610 | 0.728445 | 3.568066 |

31

**Product** scf done: -893.247105 Sum of electronic and thermal Free Energies -893.058571 imag. freq.: 0

| | | | |
|---|---|---|---|
| C | 0.002107 | -0.070925 | -0.000219 |
| C | -0.003250 | 0.021180 | 1.391952 |
| C | 1.188810 | 0.096185 | 2.113831 |
| C | 2.395683 | 0.070412 | 1.431061 |
| C | 2.419593 | -0.015594 | 0.034969 |
| C | 1.214875 | -0.082663 | -0.674886 |
| N | -1.244298 | 0.041811 | 2.082100 |
| C | -1.525128 | -0.380616 | 3.341059 |
| C | -2.872458 | -0.128536 | 3.507848 |
| N | -3.332803 | 0.431361 | 2.344393 |
| N | -2.359946 | 0.534577 | 1.489019 |
| C | -3.740714 | -0.384343 | 4.661165 |
| C | -5.127530 | -0.201910 | 4.560116 |
| C | -5.952894 | -0.445375 | 5.654419 |
| C | -5.409543 | -0.876576 | 6.864671 |
| C | -4.030671 | -1.061232 | 6.972803 |
| C | -3.201521 | -0.815360 | 5.882379 |
| C | 3.736446 | -0.030658 | -0.648163 |
| O | 4.808478 | 0.017777 | -0.081281 |
| O | 3.635249 | -0.104170 | -1.991175 |
| H | -0.786670 | -0.829233 | 3.981650 |
| H | -5.554906 | 0.128328 | 3.621672 |
| H | -7.023178 | -0.299826 | 5.560530 |
| H | -6.053716 | -1.066747 | 7.715467 |
| H | -3.598517 | -1.393870 | 7.909769 |
| H | -2.131544 | -0.955608 | 5.983927 |
| H | 1.174850 | 0.187463 | 3.191813 |

| | | | |
|---|---|---|---|
| H | 3.327339 | 0.129313 | 1.978510 |
| H | 1.221894 | -0.154849 | -1.753838 |
| H | -0.930719 | -0.140583 | -0.542221 |
| H | 4.535667 | -0.109589 | -2.360501 |

31

**$TS_{T1}$** scf done: -893.049447 Sum of electronic and thermal Free Energies -892.875247 imag. freq.: 1(-591.64)

| | | | |
|---|---|---|---|
| C | -0.295630 | 0.264754 | 0.483484 |
| C | -0.077038 | -0.458520 | 1.664705 |
| C | 1.234881 | -0.593553 | 2.151775 |
| C | 2.299051 | -0.014738 | 1.470196 |
| C | 2.073164 | 0.705484 | 0.295459 |
| C | 0.774692 | 0.844014 | -0.192948 |
| C | -1.172708 | -1.052578 | 2.408208 |
| C | -1.549023 | -1.411742 | 3.548074 |
| N | -3.794467 | 0.016644 | 1.880866 |
| N | -3.540827 | -1.118573 | 1.168189 |
| N | -2.437573 | -1.607669 | 1.084828 |
| C | -5.041973 | 0.087879 | 2.407488 |
| C | -5.995706 | -0.968286 | 2.394017 |
| C | -7.224249 | -0.789658 | 2.992226 |
| C | -7.541163 | 0.429813 | 3.619932 |
| C | -6.603060 | 1.475967 | 3.642185 |
| C | -5.370636 | 1.313670 | 3.048863 |
| C | -8.858193 | 0.655585 | 4.268224 |
| O | -9.667533 | -0.419131 | 4.206457 |
| O | -9.188840 | 1.693855 | 4.801437 |
| H | -2.240504 | -1.845977 | 4.240677 |
| H | 1.406281 | -1.155886 | 3.061706 |
| H | 3.306668 | -0.127965 | 1.853664 |
| H | 2.904793 | 1.155256 | -0.234752 |
| H | 0.592371 | 1.405486 | -1.101978 |
| H | -1.301497 | 0.383783 | 0.101684 |
| H | -4.634321 | 2.107593 | 3.057561 |
| H | -6.859607 | 2.407685 | 4.128871 |
| H | -7.948616 | -1.592582 | 2.979806 |
| H | -5.749254 | -1.905771 | 1.913948 |
| H | -10.507576 | -0.193589 | 4.643336 |

31

**IntT** scf done: -893.073082 Sum of electronic and thermal Free Energies -892.895668 imag. freq.: 0

| | | | |
|---|---|---|---|
| C | 0.414081 | -0.165641 | -0.241307 |
| C | 0.291231 | -0.075777 | 1.153510 |
| C | 1.442607 | 0.010574 | 1.956639 |
| C | 2.692881 | 0.017409 | 1.363194 |
| C | 2.816200 | -0.066029 | -0.033114 |
| C | 1.668662 | -0.157822 | -0.829198 |
| N | -1.018383 | -0.125287 | 1.650372 |
| N | -1.154621 | 0.173045 | 2.879417 |
| N | -2.321256 | 0.030378 | 3.444845 |
| C | 4.139502 | -0.065742 | -0.704696 |

| | | | |
|---|---|---|---|
| O | 4.302462 | -0.138147 | -1.905257 |
| O | 5.172553 | 0.023830 | 0.157847 |
| C | -3.148849 | -1.023871 | 3.126065 |
| C | -2.704094 | -2.168795 | 2.548862 |
| C | -4.560529 | -0.876248 | 3.554222 |
| C | -5.113824 | 0.398218 | 3.735222 |
| C | -6.447085 | 0.536645 | 4.109320 |
| C | -7.242050 | -0.593382 | 4.305448 |
| C | -6.697241 | -1.865534 | 4.125719 |
| C | -5.364147 | -2.007518 | 3.754676 |
| H | -1.784219 | -2.601070 | 2.188196 |
| H | -4.937335 | -2.996108 | 3.628562 |
| H | -7.309062 | -2.746465 | 4.282138 |
| H | -8.280154 | -0.483321 | 4.597538 |
| H | -6.867400 | 1.526730 | 4.243488 |
| H | -4.499273 | 1.275455 | 3.575278 |
| H | -0.482942 | -0.239346 | -0.843858 |
| H | 1.769796 | -0.223759 | -1.904652 |
| H | 3.578646 | 0.082770 | 1.980630 |
| H | 1.346163 | 0.067683 | 3.032650 |
| H | 5.996747 | 0.016125 | -0.359373 |

31

**$TS_{T2}$** scf done: -893.064411 Sum of electronic and thermal Free Energies -892.885787 imag. freq.: 1(-406.46)

| | | | |
|---|---|---|---|
| C | 0.097094 | -0.916261 | 0.331459 |
| C | 0.296450 | 0.162316 | 1.207510 |
| C | 1.578976 | 0.719965 | 1.322627 |
| C | 2.637975 | 0.210717 | 0.576733 |
| C | 2.431276 | -0.860828 | -0.291275 |
| C | 1.158080 | -1.422011 | -0.410865 |
| C | -0.827219 | 0.709095 | 1.997163 |
| N | -2.069676 | 0.423250 | 1.596653 |
| N | -3.034569 | 0.779268 | 2.513276 |
| N | -2.698501 | 1.779113 | 3.210356 |
| C | -0.643705 | 1.507615 | 3.135989 |
| C | -3.508417 | 2.158914 | 4.294244 |
| C | -4.857381 | 1.787322 | 4.396164 |
| C | -5.606461 | 2.234269 | 5.473097 |
| C | -5.021861 | 3.045740 | 6.456006 |
| C | -3.676200 | 3.416145 | 6.341870 |
| C | -2.922845 | 2.985491 | 5.262259 |
| C | -5.791340 | 3.540609 | 7.623462 |
| O | -7.077995 | 3.135396 | 7.621255 |
| O | -5.334356 | 4.239845 | 8.504199 |
| H | 0.190806 | 1.556508 | 3.828451 |
| H | 1.745393 | 1.562958 | 1.982503 |
| H | 3.622762 | 0.653534 | 0.670543 |
| H | 3.257200 | -1.259000 | -0.869543 |
| H | 0.995018 | -2.260715 | -1.077965 |
| H | -0.886562 | -1.360000 | 0.250073 |
| H | -1.882862 | 3.268184 | 5.160371 |

H -3.230916 4.046905 7.100227
H -6.647998 1.953239 5.552181
H -5.305870 1.168085 3.631249
H -7.510298 3.504301 8.411164

31

**$P_T$** scf done: -893.142156 Sum of electronic and thermal Free Energies -892.958671 imag. freq.: 0

C -0.019291 0.157677 0.026029
C -0.004400 -0.048126 1.428820
C 1.241182 -0.140296 2.101105
C 2.420961 -0.030170 1.392203
C 2.391411 0.173313 0.004711
C 1.170116 0.266337 -0.672068
C -1.224817 -0.161410 2.157223
C -2.562180 -0.096237 1.658505
N -3.357719 -0.258086 2.736094
N -2.483471 -0.427236 3.930227
N -1.258550 -0.358201 3.504493
C -4.711505 -0.285934 2.874265
C -5.294241 -0.477218 4.159605
C -6.663763 -0.504754 4.294444
C -7.513262 -0.345885 3.175120
C -6.922754 -0.155914 1.899479
C -5.560488 -0.125031 1.741331
C -8.966231 -0.369574 3.282453
O -9.416992 -0.557829 4.553725
O -9.749765 -0.237796 2.351311
H -2.929072 0.046796 0.659188
H 1.251556 -0.297350 3.171401
H 3.371269 -0.100910 1.907318
H 3.320439 0.259013 -0.546519
H 1.155577 0.423586 -1.743615
H -0.962372 0.230042 -0.499913
H -5.133667 0.021386 0.757960
H -7.566701 -0.033436 1.037703
H -7.094074 -0.650860 5.276419
H -4.656601 -0.599790 5.022599
H -10.387843 -0.557888 4.516989

31

**$TS_{R1}^-$** scf done: -893.226613 Sum of electronic and thermal Free Energies -893.052265 imag. freq.: 1(-432.48)

C 0.718499 -1.024618 -0.210518
C 0.293119 -0.505996 1.038527
C 1.217707 0.283031 1.770514
C 2.481660 0.537980 1.272039
C 2.893354 0.020934 0.030060
C 1.982711 -0.766448 -0.698781
N -0.984950 -0.834324 1.434357
N -1.354843 -0.253665 2.574993
N -2.386907 -0.381142 3.188884
C 4.223900 0.270681 -0.526319

| | | | |
|---|---|---|---|
| O | 4.635328 | -0.145416 | -1.597545 |
| O | 5.012647 | 1.038224 | 0.271852 |
| C | -3.659300 | -1.763746 | 2.612264 |
| C | -3.206980 | -2.710283 | 1.915237 |
| C | -4.888609 | -1.328549 | 3.264734 |
| C | -5.259077 | 0.023342 | 3.311179 |
| C | -6.455633 | 0.409988 | 3.910387 |
| C | -7.297362 | -0.543054 | 4.483830 |
| C | -6.935252 | -1.890570 | 4.448694 |
| C | -5.743706 | -2.281230 | 3.844882 |
| H | -2.326979 | -3.092237 | 1.437420 |
| H | -5.463261 | -3.327606 | 3.817672 |
| H | -7.581091 | -2.639203 | 4.894147 |
| H | -8.225460 | -0.239473 | 4.954837 |
| H | -6.730042 | 1.458889 | 3.929875 |
| H | -4.606691 | 0.766409 | 2.871345 |
| H | 0.023589 | -1.630914 | -0.780650 |
| H | 2.286019 | -1.171141 | -1.656940 |
| H | 3.166460 | 1.144220 | 1.851887 |
| H | 0.925903 | 0.686646 | 2.731219 |
| H | 5.863500 | 1.146947 | -0.184309 |

31

**$TS_{R4}^-$** scf done: -893.229501 Sum of electronic and thermal Free Energies -893.052863 imag. freq.: 1(-437.83)

| | | | |
|---|---|---|---|
| C | -0.020575 | -0.142069 | -0.066631 |
| C | 0.017524 | -0.037380 | 1.337261 |
| C | 1.268987 | 0.029335 | 1.977709 |
| C | 2.437339 | 0.030158 | 1.240910 |
| C | 2.400442 | -0.056078 | -0.159396 |
| C | 1.154812 | -0.156876 | -0.799340 |
| N | -1.111658 | 0.067613 | 2.147794 |
| N | -2.276907 | -0.340869 | 1.542911 |
| N | -3.379351 | -0.187700 | 1.963507 |
| C | 3.668428 | -0.023228 | -0.903348 |
| O | 3.510281 | -0.114550 | -2.247222 |
| O | 4.774120 | 0.080079 | -0.402776 |
| C | -1.335188 | 1.653495 | 3.047315 |
| C | -0.468055 | 2.570067 | 3.082912 |
| C | 0.817100 | 3.023296 | 2.674968 |
| C | 1.040526 | 3.499038 | 1.361031 |
| C | 2.303830 | 3.911845 | 0.955518 |
| C | 3.386218 | 3.880181 | 1.839254 |
| C | 3.174402 | 3.440707 | 3.148934 |
| C | 1.913808 | 3.032678 | 3.568413 |
| H | -0.975444 | -0.192248 | -0.573642 |
| H | 1.107829 | -0.226948 | -1.878476 |
| H | 4.395039 | -0.073494 | -2.647337 |
| H | 3.394510 | 0.101750 | 1.741725 |
| H | 1.302903 | 0.096744 | 3.056871 |
| H | -2.343923 | 1.464312 | 3.379597 |
| H | 0.215569 | 3.509258 | 0.657851 |

| | | | |
|---|---|---|---|
| H | 2.448320 | 4.251436 | -0.065011 |
| H | 4.371263 | 4.196156 | 1.515927 |
| H | 4.001322 | 3.415810 | 3.851285 |
| H | 1.766723 | 2.690227 | 4.586680 |

31

**$TS_{R3}^-$** scf done: -893.225754 Sum of electronic and thermal Free Energies -893.05079 imag. freq.: 1(-389.46)

| | | | |
|---|---|---|---|
| C | 0.592805 | -0.574318 | 0.077096 |
| C | 0.294688 | -0.098806 | 1.374089 |
| C | 1.368808 | 0.060482 | 2.277084 |
| C | 2.674765 | -0.224622 | 1.892804 |
| C | 2.954262 | -0.695574 | 0.607338 |
| C | 1.901509 | -0.868210 | -0.294017 |
| C | -1.053855 | 0.188828 | 1.753072 |
| C | -1.972783 | 1.027671 | 1.538010 |
| N | -1.664112 | 2.569795 | 0.471628 |
| N | -0.857292 | 3.537681 | 0.995640 |
| N | -0.036368 | 3.408699 | 1.844713 |
| C | -2.699329 | 3.041514 | -0.315505 |
| C | -3.025864 | 4.407447 | -0.478152 |
| C | -4.085157 | 4.786588 | -1.283194 |
| C | -4.872640 | 3.828091 | -1.943228 |
| C | -4.556391 | 2.470126 | -1.774859 |
| C | -3.492801 | 2.080461 | -0.983650 |
| C | -6.008013 | 4.193930 | -2.798685 |
| O | -6.726964 | 3.408510 | -3.392082 |
| O | -6.209559 | 5.533044 | -2.886028 |
| H | -2.438807 | 5.159997 | 0.031214 |
| H | -4.312689 | 5.838897 | -1.396433 |
| H | -6.975496 | 5.674745 | -3.467413 |
| H | -5.152676 | 1.722217 | -2.283184 |
| H | -3.248741 | 1.030864 | -0.877501 |
| H | -3.010618 | 1.213095 | 1.751805 |
| H | 1.165704 | 0.417338 | 3.280501 |
| H | 3.481322 | -0.082978 | 2.604666 |
| H | 3.972666 | -0.923599 | 0.314460 |
| H | 2.101171 | -1.229968 | -1.297383 |
| H | -0.215084 | -0.709009 | -0.633367 |

31

**$int_R^-$** scf done: -893.246517 Sum of electronic and thermal Free Energies -893.068052 imag. freq.: 0

| | | | |
|---|---|---|---|
| C | -0.102535 | -0.190391 | 0.176931 |
| C | 0.180484 | 0.007579 | 1.536702 |
| C | 1.513938 | 0.218444 | 1.914350 |
| C | 2.533077 | 0.219340 | 0.962779 |
| C | 2.239665 | 0.016684 | -0.385322 |
| C | 0.914478 | -0.187469 | -0.773816 |
| C | -0.914723 | -0.025406 | 2.555903 |
| C | -2.001262 | -0.766677 | 2.352292 |
| N | -0.599913 | 0.802464 | 3.687396 |
| N | -1.384149 | 0.908563 | 4.691103 |
| N | -2.508930 | 0.238450 | 4.730305 |

| | | | |
|---|---|---|---|
| C | -3.283585 | 0.489580 | 5.855208 |
| C | -4.434587 | -0.314004 | 6.019263 |
| C | -5.281927 | -0.136959 | 7.095906 |
| C | -5.021347 | 0.852194 | 8.059388 |
| C | -3.880676 | 1.658933 | 7.902363 |
| C | -3.028521 | 1.487905 | 6.825735 |
| C | -5.948534 | 1.007005 | 9.186764 |
| O | -5.595036 | 1.994051 | 10.048878 |
| O | -6.950788 | 0.338211 | 9.372955 |
| H | -2.918454 | -1.004787 | 2.858868 |
| H | -1.131412 | -0.338923 | -0.130659 |
| H | 0.671757 | -0.336595 | -1.820331 |
| H | 3.032369 | 0.021368 | -1.125066 |
| H | 3.559124 | 0.376631 | 1.277296 |
| H | 1.749070 | 0.374806 | 2.958968 |
| H | -4.640199 | -1.080190 | 5.280542 |
| H | -6.158112 | -0.764167 | 7.206845 |
| H | -3.665976 | 2.429906 | 8.631765 |
| H | -2.160667 | 2.123623 | 6.717390 |
| H | -6.265058 | 2.016875 | 10.752482 |

31

**$TS_{R2}^-$** scf done: -893.247530 Sum of electronic and thermal Free Energies -893.067532 imag. Freq.: 1(-201.45)

| | | | |
|---|---|---|---|
| C | 0.139033 | 0.467624 | -0.116572 |
| C | -0.119843 | -0.542153 | 0.844241 |
| C | 0.987846 | -1.189258 | 1.452429 |
| C | 2.279206 | -0.859834 | 1.089929 |
| C | 2.531333 | 0.138531 | 0.127503 |
| C | 1.432598 | 0.796707 | -0.462542 |
| N | -1.420231 | -0.778410 | 1.200125 |
| N | -1.737291 | -1.953984 | 1.688212 |
| N | -2.856160 | -2.055866 | 2.313339 |
| C | -3.590209 | -0.853923 | 2.461090 |
| C | -3.040361 | 0.318040 | 2.121641 |
| C | 3.884590 | 0.516526 | -0.274843 |
| O | 4.169382 | 1.365742 | -1.106020 |
| C | -4.957440 | -1.035917 | 3.024329 |
| C | -5.997665 | -0.155215 | 2.692115 |
| C | -7.267940 | -0.311161 | 3.240180 |
| C | -7.526662 | -1.351328 | 4.134847 |
| C | -6.501043 | -2.234749 | 4.470771 |
| C | -5.230420 | -2.081782 | 3.918453 |
| O | 4.859927 | -0.178744 | 0.371255 |
| H | -3.519503 | 1.290902 | 2.047465 |
| H | -4.438688 | -2.771106 | 4.183435 |
| H | -6.689318 | -3.046116 | 5.165592 |
| H | -8.515660 | -1.472090 | 4.562371 |
| H | -8.059654 | 0.376663 | 2.963708 |
| H | -5.809241 | 0.650661 | 1.992027 |
| H | -0.701482 | 0.973165 | -0.578089 |
| H | 1.617210 | 1.566458 | -1.202139 |

| | | | |
|---|---|---|---|
| H | 3.110207 | -1.372033 | 1.558481 |
| H | 0.807273 | -1.942118 | 2.209295 |
| H | 5.712406 | 0.140783 | 0.032135 |

31

$\mathbf{P_R}^-$ scf done: -893.339457 Sum of electronic and thermal Free Energies -893.155112 imag. freq.: 0

| | | | |
|---|---|---|---|
| C | 0.021533 | 0.158680 | -0.031468 |
| C | -0.040561 | -0.081882 | 1.366836 |
| C | 1.168828 | -0.291659 | 2.080515 |
| C | 2.376720 | -0.262392 | 1.425039 |
| C | 2.461710 | -0.023052 | 0.019623 |
| C | 1.233581 | 0.186397 | -0.680258 |
| N | -1.271370 | -0.112327 | 2.024171 |
| C | -1.535967 | -0.333445 | 3.348330 |
| C | -2.918174 | -0.257569 | 3.459298 |
| N | -3.429460 | 0.000643 | 2.228770 |
| N | -2.447160 | 0.091792 | 1.349586 |
| C | -3.761296 | -0.415423 | 4.648179 |
| C | -5.160621 | -0.369952 | 4.544633 |
| C | -5.961329 | -0.520934 | 5.672888 |
| C | -5.383310 | -0.721554 | 6.927699 |
| C | -3.993698 | -0.768842 | 7.041308 |
| C | -3.189519 | -0.617160 | 5.914591 |
| C | 3.741244 | -0.001033 | -0.620710 |
| O | 4.844908 | -0.172756 | -0.082417 |
| O | 3.688727 | 0.240644 | -1.981188 |
| H | -0.767250 | -0.521420 | 4.074211 |
| H | -5.615633 | -0.217273 | 3.573942 |
| H | -7.040453 | -0.483300 | 5.572234 |
| H | -6.008216 | -0.839521 | 7.805576 |
| H | -3.532678 | -0.923484 | 8.010548 |
| H | -2.111633 | -0.654058 | 6.021947 |
| H | 1.150400 | -0.476395 | 3.147199 |
| H | 3.291485 | -0.424098 | 1.982577 |
| H | 1.255993 | 0.371398 | -1.746787 |
| H | -0.893524 | 0.319936 | -0.584820 |
| H | 4.607707 | 0.230183 | -2.289214 |

31

$\mathbf{P_{R2}}^-$ scf done: -893.328998 Sum of electronic and thermal Free Energies -893.159232 imag. freq.: 0

| | | | |
|---|---|---|---|
| C | -0.728693 | -0.799917 | 0.279316 |
| C | 0.189720 | -0.747917 | 1.379493 |
| C | 1.378537 | -1.542219 | 1.269722 |
| C | 1.613903 | -2.325904 | 0.153644 |
| C | 0.694974 | -2.362024 | -0.904998 |
| C | -0.474312 | -1.591778 | -0.826683 |
| C | -0.038879 | 0.062294 | 2.469908 |
| C | -0.424693 | 0.585349 | 3.625048 |
| N | -0.287010 | 1.833601 | 4.200529 |
| N | -2.473903 | 2.944485 | 2.066594 |
| N | -1.988341 | 2.579708 | 1.154523 |
| C | 0.424802 | 2.813981 | 3.609131 |

| | | | |
|---|---|---|---|
| C | 0.461558 | 4.086491 | 4.270694 |
| C | 1.137298 | 5.166243 | 3.756176 |
| C | 1.845761 | 5.067844 | 2.532945 |
| C | 1.833750 | 3.826134 | 1.870844 |
| C | 1.154347 | 2.735894 | 2.377791 |
| C | 2.572172 | 6.182819 | 1.949386 |
| O | 3.204456 | 6.165090 | 0.900218 |
| O | 2.504383 | 7.329419 | 2.688865 |
| H | -0.078483 | 4.179330 | 5.207298 |
| H | 1.128278 | 6.107218 | 4.292683 |
| H | 3.016667 | 8.002569 | 2.212302 |
| H | 2.372889 | 3.730859 | 0.934665 |
| H | 1.172601 | 1.806027 | 1.827045 |
| H | -0.991516 | -0.098956 | 4.271054 |
| H | 2.094606 | -1.517012 | 2.083013 |
| H | 2.520842 | -2.918917 | 0.099460 |
| H | 0.887450 | -2.977606 | -1.775829 |
| H | -1.189174 | -1.614222 | -1.642557 |
| H | -1.631668 | -0.203214 | 0.329951 |

31

**$TS_{T1nitrogen}$** scf done: -893.088100 Sum of electronic and thermal Free Energies -892.917184 imag. freq.: 1 (-250.92)

| | | | |
|---|---|---|---|
| C | -0.022403 | 0.071122 | 0.075229 |
| C | 0.019312 | 0.023401 | 1.468956 |
| C | 1.248637 | -0.007548 | 2.127906 |
| C | 2.433887 | 0.014730 | 1.401111 |
| C | 2.398521 | 0.070104 | -0.002483 |
| C | 1.157157 | 0.091128 | -0.660543 |
| C | 3.611463 | 0.094492 | -0.752683 |
| C | 4.637148 | 0.101106 | -1.386656 |
| N | 0.623149 | -3.233670 | 1.307336 |
| N | 1.327463 | -3.182790 | 0.386742 |
| N | 2.824223 | -3.289988 | 0.549691 |
| C | 3.443873 | -3.261075 | -0.640101 |
| C | 2.817459 | -3.121401 | -1.917052 |
| C | 3.584422 | -3.095514 | -3.058403 |
| C | 4.986766 | -3.203424 | -2.982349 |
| C | 5.616714 | -3.342350 | -1.733076 |
| C | 4.868915 | -3.370653 | -0.579823 |
| C | 5.840528 | -3.162530 | -4.196400 |
| O | 5.133125 | -3.039873 | -5.335834 |
| O | 7.051815 | -3.229687 | -4.182193 |
| H | 5.543502 | 0.100005 | -1.947236 |
| H | 1.129445 | 0.123494 | -1.742900 |
| H | -0.975916 | 0.086815 | -0.439891 |
| H | -0.902312 | 0.003061 | 2.038957 |
| H | 1.284357 | -0.053335 | 3.210172 |
| H | 3.390242 | -0.011701 | 1.908876 |
| H | 5.338363 | -3.469818 | 0.390738 |
| H | 6.695053 | -3.420492 | -1.688852 |
| H | 3.105798 | -2.984213 | -4.021763 |

H 1.742635 -3.028755 -1.975360
H 5.759814 -3.017032 -6.080461

31

**$T_{1azide}$** scf done: -893.088128 Sum of electronic and thermal Free Energies -892.916767 imag. freq.: 0

C 0.040076 -0.040320 -0.058676
C -0.002250 -0.027733 1.368844
C 1.227067 0.009401 2.096048
C 2.428471 0.030994 1.427352
C 2.455874 0.019333 0.021941
C 1.252127 -0.017863 -0.708613
N -1.111621 -0.035688 2.128727
N -2.327669 -0.088054 1.311658
N -3.386736 -0.150109 1.799730
C 3.778211 0.059921 -0.652928
O 4.840906 0.111804 -0.070113
O 3.686501 0.035370 -1.996153
C -4.174738 3.031922 1.321164
C -3.393539 3.168771 2.468942
C -2.009842 3.261570 2.367635
C -1.391547 3.219268 1.106527
C -2.183233 3.071675 -0.044950
C -3.566181 2.982338 0.066636
C 0.027478 3.313180 0.997065
C 1.228143 3.377933 0.906351
H 2.289689 3.428259 0.826790
H -1.706065 3.028534 -1.016415
H -4.169867 2.867676 -0.826214
H -5.252744 2.956837 1.404542
H -3.862725 3.198960 3.445469
H -1.399579 3.365099 3.256448
H 1.186562 0.025379 3.177862
H 3.360729 0.063432 1.975639
H 1.279729 -0.022038 -1.789676
H -0.883788 -0.059766 -0.618730
H 4.588028 0.067904 -2.362175

14

**$C^+$** scf done: -308.277539 Sum of electronic and thermal Free Energies -308.200902 imag. freq.: 0

C -0.015130 0.000750 -0.029317
C 0.001856 0.000952 1.405449
C 1.248404 0.000458 2.115987
C 2.422294 -0.000366 1.410624
C 2.391507 -0.000650 -0.002087
C 1.170943 -0.000081 -0.714019
C -1.191694 0.001846 2.108263
C -2.242305 0.002762 2.725670
H 1.233156 0.000743 3.197699
H 3.374100 -0.000777 1.925401
H 3.325204 -0.001279 -0.551998
H 1.182208 -0.000284 -1.796057
H -0.968585 0.001254 -0.540464

H -3.164565 0.004009 3.268360

31

**$TS_C^+$** scf done: -892.885885 Sum of electronic and thermal Free Energies -892.707358 imag. freq.: 1 (-278.50)

C 0.723042 1.161395 0.595628
C 0.088166 0.132997 1.310907
C 0.670853 -1.141294 1.363503
C 1.880194 -1.376888 0.718621
C 2.509014 -0.354360 0.007146
C 1.927332 0.912199 -0.053849
C -1.139957 0.427636 2.003933
C -1.916636 1.092178 2.692234
N -3.857101 -0.153141 2.670373
N -3.391448 -1.096544 1.897017
N -2.355403 -1.263844 1.416645
C -5.151444 -0.117277 3.022787
C -6.124593 -1.077869 2.603424
C -7.419680 -0.939855 3.026398
C -7.783562 0.140494 3.862704
C -6.825952 1.090277 4.275648
C -5.523462 0.975272 3.867488
C -9.189560 0.317193 4.336860
O -10.011907 -0.637639 3.882114
O -9.542957 1.225882 5.053442
H -2.414912 1.789444 3.326910
H 0.179558 -1.935538 1.911124
H 2.330045 -2.361574 0.767579
H 3.448094 -0.544732 -0.499405
H 2.411851 1.708261 -0.607034
H 0.267717 2.143148 0.554964
H -4.765567 1.687410 4.165379
H -7.131234 1.907094 4.915337
H -8.166069 -1.658222 2.717740
H -5.823604 -1.894893 1.960374
H -10.908911 -0.465960 4.222196

31

**$P_C^+$** scf done: -893.025489 Sum of electronic and thermal Free Energies -892.837477 imag. freq.: 0

C -0.054829 0.638237 0.198387
C 0.863533 1.118638 1.179780
C 1.985390 0.384800 1.483490
C 2.223566 -0.837518 0.828482
C 1.326357 -1.324879 -0.140155
C 0.200295 -0.603740 -0.457586
C -1.209960 1.396411 -0.113595
C -2.244962 1.139433 -1.035920
N -3.083351 2.158223 -0.915553
C -4.290398 2.439755 -1.605729
C -4.494339 1.909275 -2.881239
C -5.683964 2.183180 -3.535583
C -6.657478 2.986079 -2.929825

| | | | |
|---|---|---|---|
| C | -6.432192 | 3.515113 | -1.654570 |
| C | -5.247561 | 3.243987 | -0.984871 |
| C | -7.913246 | 3.253984 | -3.680969 |
| O | -8.157287 | 2.813904 | -4.783899 |
| N | -2.608701 | 3.058481 | 0.062827 |
| N | -1.518133 | 2.597397 | 0.514845 |
| O | -8.769611 | 4.045561 | -3.008661 |
| H | -5.072078 | 3.638138 | 0.006078 |
| H | -7.181125 | 4.133250 | -1.179429 |
| H | -9.562206 | 4.172596 | -3.559663 |
| H | -5.859995 | 1.784758 | -4.525967 |
| H | -3.733564 | 1.307965 | -3.360742 |
| H | -2.403681 | 0.311583 | -1.706905 |
| H | 0.662923 | 2.060067 | 1.672663 |
| H | 2.687316 | 0.743130 | 2.225610 |
| H | 3.109403 | -1.411481 | 1.072810 |
| H | 1.526515 | -2.267783 | -0.632697 |
| H | -0.494000 | -0.974814 | -1.199853 |

21
Ferrocenium cation (doublet) scf done: -1650.77212275 Sum of electronic and thermal Free Energies -1650.638203 imag. freq.: 0
Fe -0.006375 -0.00275 0.019756
C 0.981306 -1.819151 -0.252573
C 0.294377 -1.451967 -1.448388
C -1.096466 -1.351197 -1.144436
C -1.268733 -1.658863 0.23809
C 0.014561 -1.948639 0.788799
C 1.416001 1.474104 0.410069
C 0.664848 1.813136 -0.754814
C -0.707703 1.921061 -0.377585
C -0.803477 1.651296 1.020178
C 0.508663 1.372978 1.50645
H 2.049769 -1.925793 -0.14289
H 0.753031 -1.23319 -2.40054
H -1.873753 -1.044093 -1.827016
H -2.198426 -1.623228 0.784894
H 0.225862 -2.167879 1.82432
H 2.476117 1.275281 0.444079
H 1.05598 1.914836 -1.755451
H -1.534649 2.116462 -1.043088
H -1.715612 1.605026 1.595373
H 0.7622 1.082957 2.514594

21
Ferrocene scf done: -1650.95721422 Sum of electronic and thermal Free Energies -1650.823183 imag. freq.: 0
Fe 0.000161 0 0
C 1.21429 0 1.677698
C 0.37521 -1.155009 1.677618

C -0.982509 -0.713823 1.675533
C -0.982509 0.713823 1.675533
C 0.37521 1.155009 1.677618
C 1.21429 0 -1.677698
C 0.37521 -1.155009 -1.677618
C -0.982509 -0.713823 -1.675533
C -0.982509 0.713823 -1.675533
C 0.37521 1.155009 -1.677618
H 2.294388 0 1.651596
H 0.709007 -2.182158 1.651191
H -1.856324 -1.348584 1.648233
H -1.856324 1.348584 1.648233
H 0.709007 2.182158 1.651191
H 2.294388 0 -1.651596
H 0.709007 -2.182158 -1.651191
H -1.856324 -1.348584 -1.648233
H -1.856324 1.348584 -1.648233
H 0.709007 2.182158 -1.651191